

## Chapter 3 Crystallography and Diffraction Techniques

### 3.1 General comments on molecular and non-molecular solids

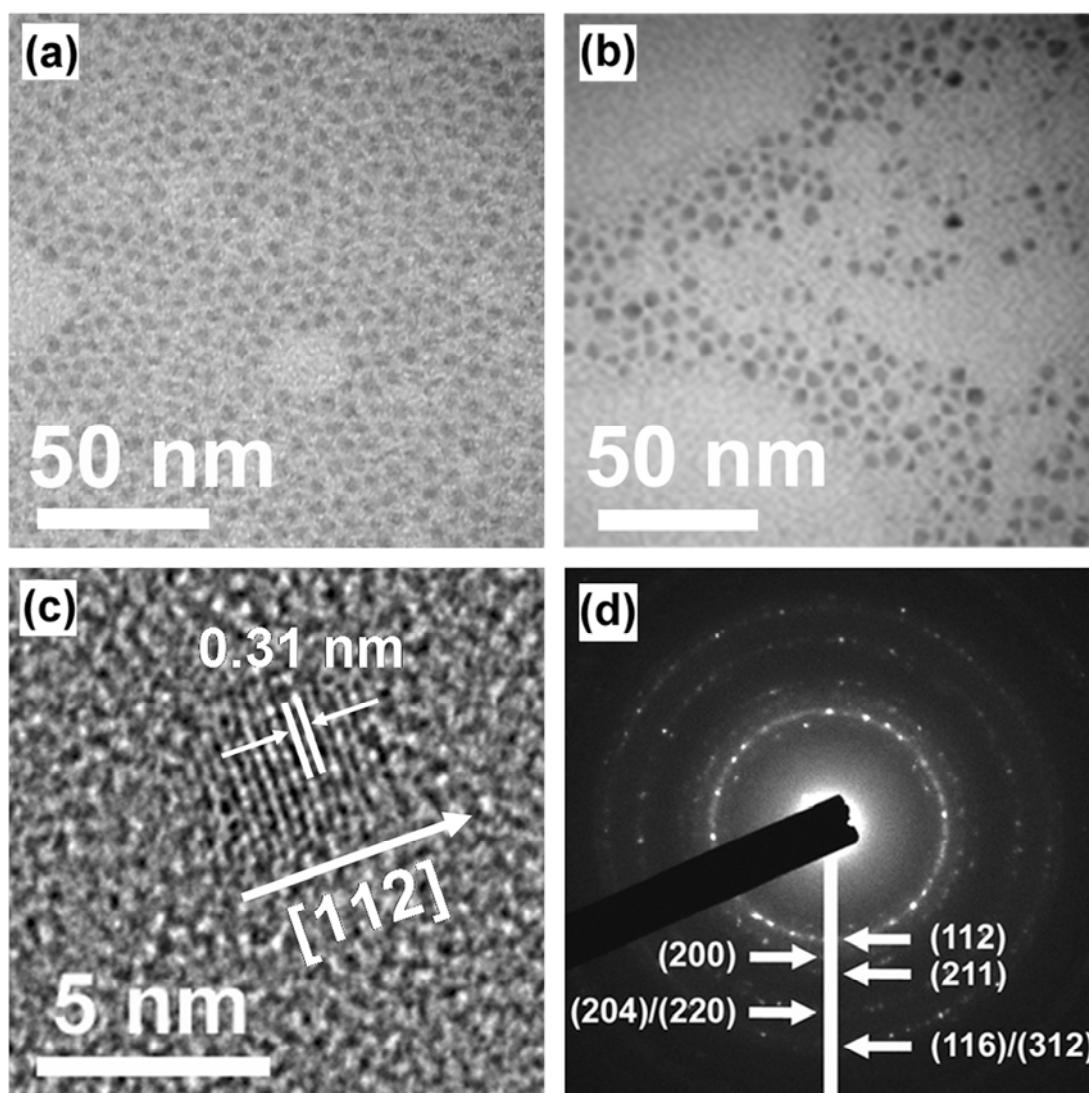
Inorganic materials and substances: molecular and non-molecular

- Identification of molecular substances—spectroscopic methods and chemical analysis
- Identification of non-molecular or crystalline substances—X-ray powder diffraction (and chemical analysis where necessary). Each crystalline solid has its own characteristic X-ray powder pattern which may be used as a “fingerprint” for its identification. (*Powder Diffraction File*)

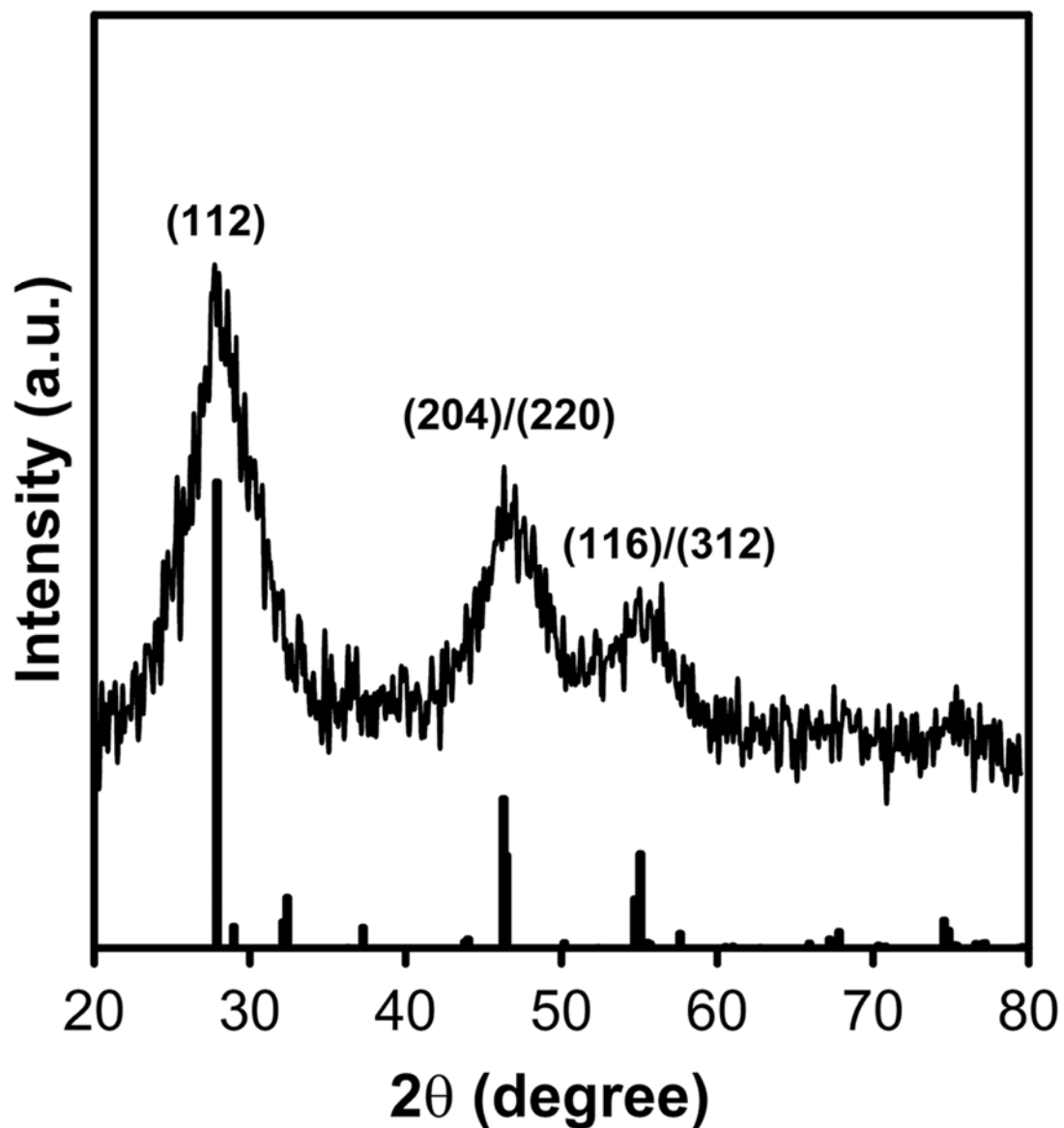
After identification of the substances, the next stage is to determine its structure.

- molecular substances— further spectroscopic measurements; X-ray crystallography if the substance is crystalline (the molecules are packed together).
- non-molecular substances— ‘structure’ takes on a whole new meaning. We need to know the crystal structure (i.e. the unit cell and its content). Defects and impurities are often extremely important and sometimes control properties. E.g. color and lasing action of ruby, Cr-doped  $\text{Al}_2\text{O}_3$ , depend on the presence of  $\text{Cr}^{3+}$  impurities.  $\therefore$  the crystal structure of the host is important but the local structure centered on the impurities or defects control the properties.

Properties of non-molecular nanoparticles. Optical properties depend on crystallite size. E.g. the color, band gap, photoconductivity of CdS nanoparticles depends on the size.



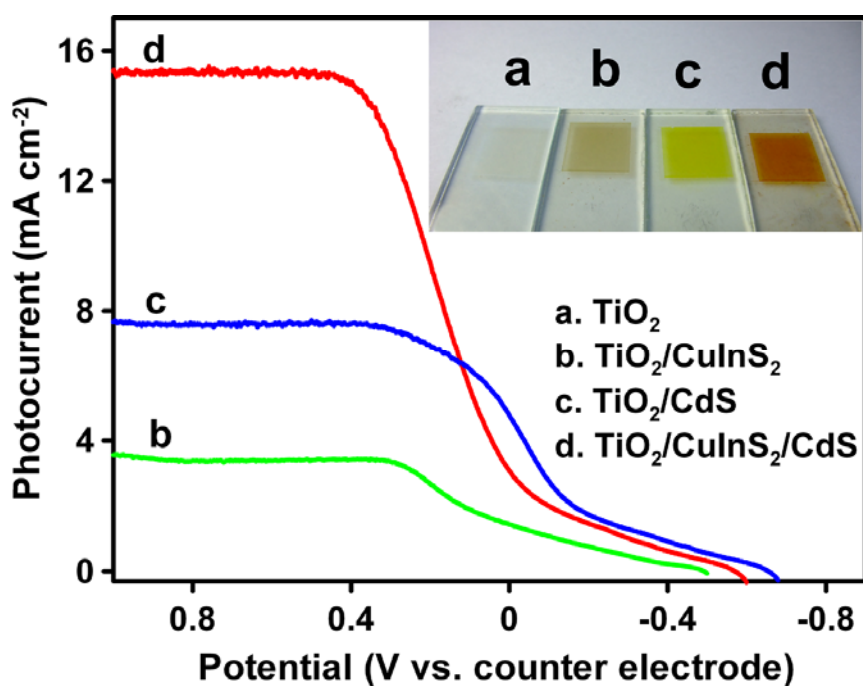
TEM images of the as-prepared  $\text{CuInS}_2$  QDs grown for 1 h at (a)  $150^\circ\text{C}$  and (b)  $170^\circ\text{C}$ . (c) HRTEM image of the as-prepared  $\text{CuInS}_2$  QDs grown at  $150^\circ\text{C}$  for 1 h with visible lattice fringes. (d) Selected-area electron diffraction pattern of the  $150^\circ\text{C}$   $\text{CuInS}_2$  QDs. The arrows point to where the vertical white line crosses the crystal face rings.



XRD pattern of the  $\text{CuInS}_2$  QDs grown at  $150\text{ }^\circ\text{C}$  for 1 h indexed to the tetragonal chalcopyrite crystal structure. The standard pattern of  $\text{CuInS}_2$  (JCPDS file no. 85-1575) is provided at the bottom of this figure.



Colors of the  $\text{CuInS}_2$  QDs grown at different solvothermal temperatures for 1 h. These QDs are dispersed in hexane.



$\text{CuInS}_2$  quantum dots coated with CdS effectively sensitize a  $\text{TiO}_2$  film to provide an extraordinarily high photocurrent under one-sun illumination

Mechanical and Electrical properties of ceramics (a larger scale). They are often determined by the microstructure, which covers the size, shape and distribution of crystalline grains, the bonding between grains, the segregation of any impurities to the surface.

For non-molecular materials, we are interested in materials of different sizes ranging from several angstroms to micron level.  $\therefore$  a wide range of techniques is needed to characterize the solids.

The prime reason for the great difference between molecular and non-molecular materials lies in the status of defects and impurities. In molecular materials, defects are not allowed! Molecules have accurately fixed formulae or stoichiometries and are defect-free.

In non-molecular materials, defects and impurities are almost unavoidable. Impurities give rise to non-stoichiometry, which may induce dramatic changes in properties.

Table 3.1 shows comparison of toluene and  $\text{Al}_2\text{O}_3$ . Toluene is an extremely well-understood molecule; aluminum oxide shows a rich diversity of structures, properties and applications and is still being actively researched.

Table 3.1 Comparison of a molecular substance, toluene,  $C_6H_5CH_3$ , and a non-molecular substance,  $Al_2O_3$

	Toluene	Alumina
Stoichiometry	Fixed, $C_6H_5CH_3$	Fixed, $Al_2O_3$
Impurities?	Not allowed	Readily doped
Nature of the material	Volatile liquid	Can be: powder, fibre, ceramic, single crystal, film
Properties		Depend on the nature of the material and dopants/impurities
Applications	Solvent	Abrasive (powder), thermal insulator (saffil fibres), electrical insulator (thin film or ceramic substrate), ruby gem and laser (Cr doped), solid electrolyte (Na beta-alumina)

### 3.2 Characterization of solids

Some important issues:

- (a) Crystal structure
- (b) Crystal defects
- (c) Impurities
- (d) For polycrystalline solid– the number, size, shape and distribution of the crystalline particles
- (e) The surface structure

Three main categories of physical techniques: diffraction, microscopic and spectroscopic techniques.

X-ray diffraction is the principal technique of solid state chemistry.

### 3.3 X-ray diffraction

#### a) Generation of X-rays

X-rays are electromagnetic radiation of wavelength  $\sim 1 \text{ \AA}$ , between  $\gamma$ -rays and UV. X-rays are produced when high-energy charged particles (e.g. electrons) accelerated through 30,000 V, collide with matter. The resulting X-ray spectra usually consist of *white radiation* (a broad spectrum) and a number of monochromatic wavelengths.

White radiation arises when the lost energy of the electrons (slowed down or stopped by collision) is converted into radiation. The lower wavelength limit corresponds to the X-ray highest energy and occurs when all the kinetic energy is converted into X-rays.  $\lambda_{\min} (\text{\AA}) = 12400/V$ , V is the accelerating voltage.

Monochromatic X-rays are used in almost all diffraction experiments. A beam of electrons strike a metal target (accelerated through  $\sim 30 \text{ kV}$ ), often Cu, to ionize some of the Cu 1s (K shell) electrons, Fig. 3.1a. An electron in an outer orbital (2p or 3p) immediately drops down to fill the vacant 1s with the energy released as X-radiation.

Fig. 3.1b: For Cu,  $2p \rightarrow 1s$ ,  $K_{\alpha}$  transition,  $1.5418 \text{ \AA}$  in wavelength.

$3p \rightarrow 1s$ ,  $K_{\beta}$  transition,  $1.3922 \text{ \AA}$  in wavelength.

The  $K_{\alpha}$  transition occurs much more frequently than the  $K_{\beta}$ .  $\therefore K_{\alpha}$  is used in diffraction experiments.

The  $K_{\alpha}$  transition is a doublet:  $K_{\alpha 1} = 1.54051 \text{ \AA}$ ,  $K_{\alpha 2} = 1.54433 \text{ \AA}$

The two possible spin states of the 2p electrons make this doublet. In some experiments, the diffraction by  $K_{\alpha_1}$  and  $K_{\alpha_2}$  is not resolved. In other experiments, separate diffraction peaks may be observed (this can be overcome by removing the weaker  $K_{\alpha_2}$  beam).

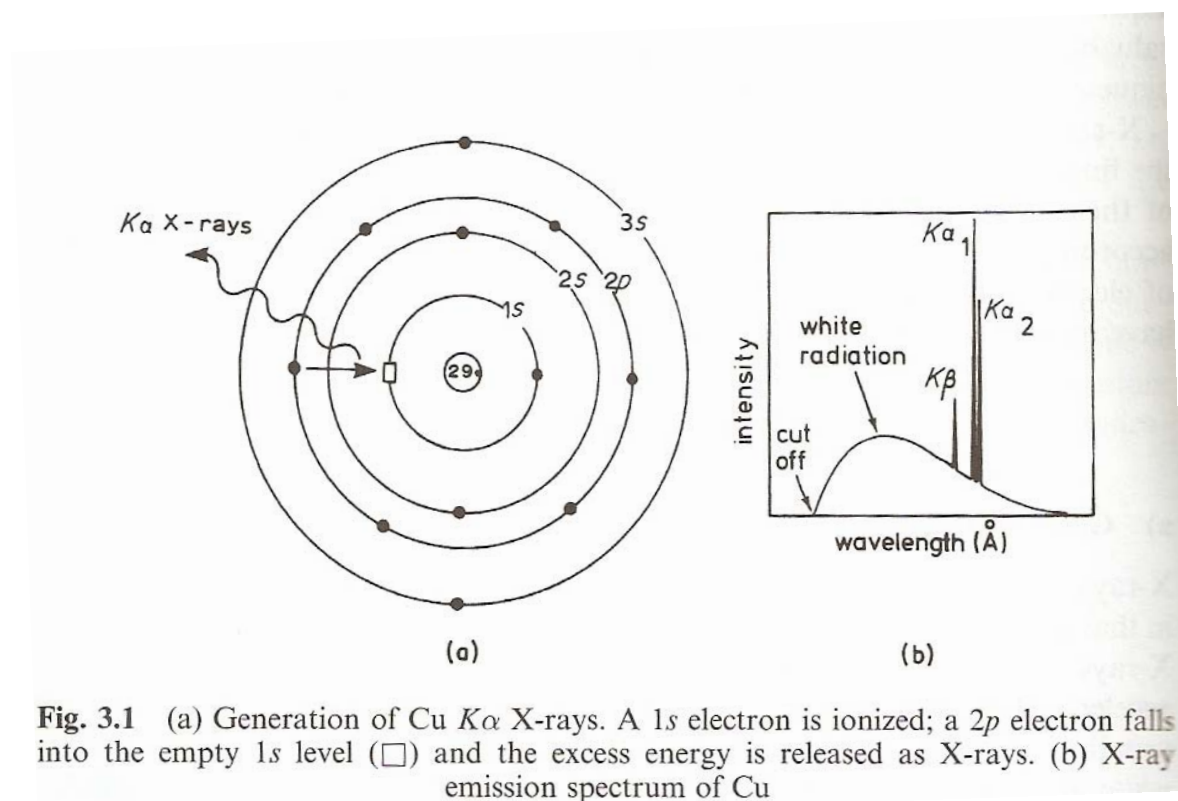


**Fig. 3.1** (a) Generation of Cu  $K_{\alpha}$  X-rays. A 1s electron is ionized; a 2p electron falls into the empty 1s level ( $\square$ ) and the excess energy is released as X-rays. (b) X-ray emission spectrum of Cu

Table 3.2 *X-ray wavelengths ( $\text{\AA}$ ) of commonly used target materials*

Target	$K_{\alpha_1}$	$K_{\alpha_2}$	$K\bar{\alpha}^*$	Filter
Cr	2.2896	2.2935	2.2909	V
Fe	1.9360	1.9399	1.9373	Mn
Cu	1.5405	1.5443	1.5418	Ni
Mo	0.7093	0.7135	0.7107	Nb
Ag	0.5594	0.5638	0.5608	Pd

\*  $\bar{\alpha}$  is the intensity-weighted average of  $\alpha_1$  and  $\alpha_2$ .

Table 3.2 shows the  $K_\alpha$  lines of different target metals.

$$\lambda^{-1/2} = C(Z - \sigma) \quad \text{Moseley's law}$$

where  $Z$  is the atomic number,  $C$  and  $\sigma$  are constants. The wavelength decreases (energy increases) with the atomic number.

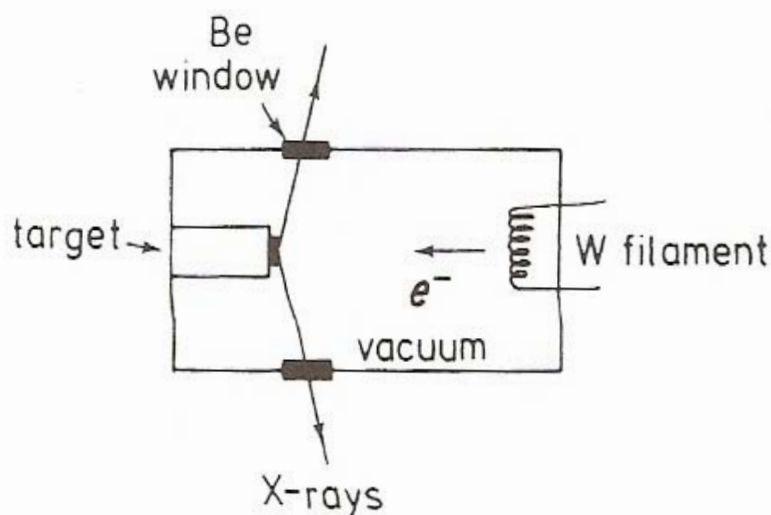


**Fig. 3.2** Schematic design of a filament X-ray tube

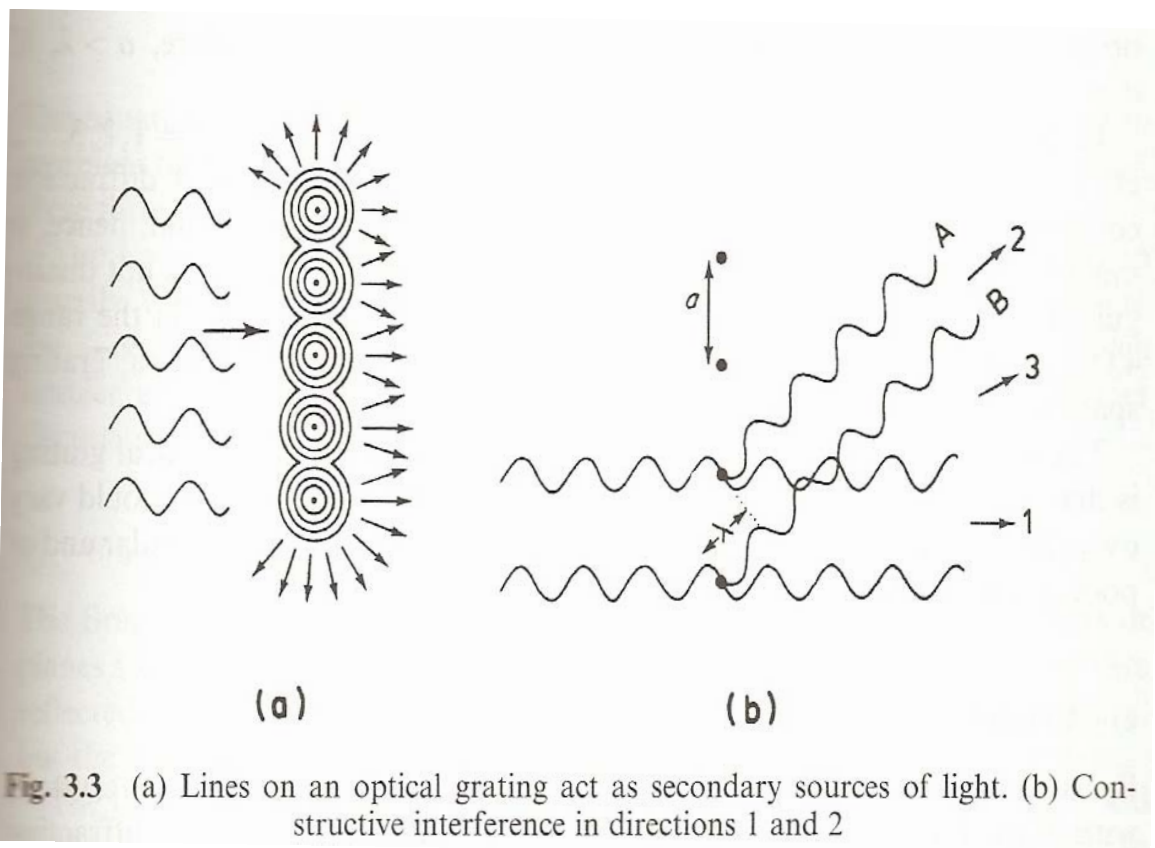
Fig. 3.2: The electron beam, provided by a heated tungsten filament, is accelerated towards an anode (attached with a piece of Cu) by a voltage of  $\sim 30$  kV. The chamber is known as the X-ray tube, is evacuated to prevent W oxidation. Be windows are very suitable for X-ray passing through, because Be has an atomic number of 4 (non-absorbing). Lead is very effective in shielding X-ray by absorbing. Continuous cooling of the anode is necessary because only a small fraction of the incident electron energy is converted to X-ray (a large fraction into heat).

A monochromatic beam of X-rays is desired for diffraction. For Cu radiation, Ni foil is a very effective filter. The energy required to ionize 1s electrons of Ni corresponds to a wavelength of  $1.488 \text{ \AA}$ , which lies

between the values for the  $K_\alpha$  and  $K_\beta$  lines of Cu (Ni absorbs  $K_\beta$  and most of the white radiation). In Table 3.2, Fe (a lighter element) would absorb Cu  $K_\alpha$  and  $K_\beta$  because its *absorption edge* is displaced to higher wavelengths. Zn (a heavier element) would transmit both Cu  $K_\alpha$  and  $K_\beta$ .

### b) An optical grating and diffraction of light

An optical grating is a piece of glass on which have been ruled a large number of parallel lines. The separation of the lines is a little larger than the wavelength of light, say  $10,000 \text{ \AA}$  (Fig. 3.3a). Consider a beam of light hitting the grating, the lines act as secondary point (or line) sources of light and re-radiate light in all direction (光必須繞過 lines 才能通過 glass). Interference occurs between the waves originating from each line source.



Constructive interference occurs in two directions as shown in Fig. 3.3b,

directions 1 and 2. Direction 1: parallel to the incident beam, diffracted beams are in phase. Direction 2: beams are in phase, although beam B is one wavelength behind beam A. Directions between 1 and 2: B lags A by a fraction of one wavelength (destructive). Complete destructive interference occurs in direction 3, because B is half a wavelength behind A.

In optical grating, there are several hundreds or thousands of beams. This causes the resultant diffracted beams to sharpen enormously after interference.  $\therefore$  Intense beams occur in directions 1 and 2, and no intensity over the whole range between 1 and 2.

The direction in which constructive interference occurs are governed by wavelength,  $\lambda$ , and the separation of lines,  $a$ . In Fig. 3.4, beams 1 and 2 (at an angle  $\phi$  to the incident direction) are in phase:

$$AB = \lambda, 2\lambda, \dots, n\lambda$$

But  $AB = a \sin\phi$

Therefore  $a \sin\phi = n\lambda$ , where  $n$  is called the diffraction order

From the above equations, we can understand why the separation of lines must be of the same order of magnitude as, but somewhat larger than, the wavelength of light. To observe 1<sup>st</sup> order diffraction, it must be that  $a > \lambda$  since  $\sin\phi < 1$ . If  $a < \lambda$ , only the zero order direct beam is observed. On the other hand, if  $a \gg \lambda$ ,  $\sin\phi$  and  $\phi$  must be very small and 1<sup>st</sup> order diffraction beam is not distinguishable from the primary beam; likewise for beams with  $n = 1, 2, \dots$ , etc.).

In order to observe well-separated spectra, grating spacings are usually

10,000–20,000 Å. The lines in an optical grating should be accurately parallel, or otherwise the diffraction spectra would be blurred.

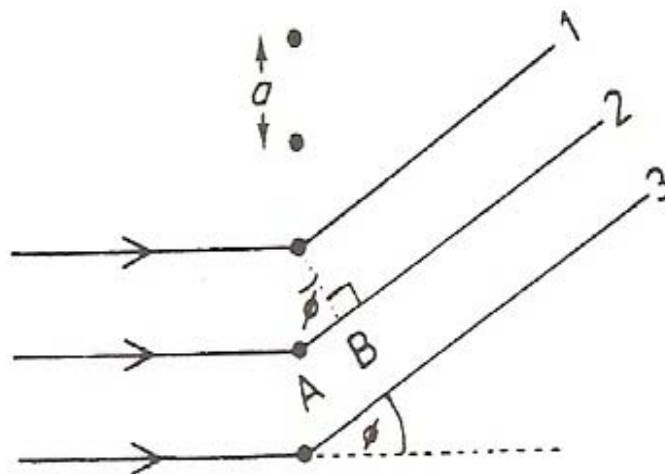


**Fig. 3.4** Diffraction of light by an optical grating

### c) Crystal and diffraction of X-rays

Crystals, with their regularly repeating structures, should be capable of diffracting radiation. Three types of radiation are used for crystal diffraction studies: X-rays, electrons and neutrons. When crystals diffract X-rays, the atoms or ions act as secondary point sources and scatter the X-rays.

Historically, two approaches have been used to treat diffraction by crystals:

#### i) The Laue equations

1 D crystal, the separation,  $a$ , of the atoms in the row, the X-ray wavelength,  $\lambda$ , and the diffraction angle,  $\phi$ ; i.e.

$$a \sin \phi = n \lambda$$

A real crystal is a 3D arrangement for which three Laue equations may be:

$$a_1 \sin \phi_1 = n \lambda$$

$$a_2 \sin \phi_2 = n \lambda$$

$$a_3 \sin \phi_3 = n \lambda$$

For a diffraction beam to occur, these three equations must be satisfied simultaneously. The Laue equations provide a rigorous and mathematically correct way to describe diffraction by crystals. However, they are cumbersome to use.

## ii) Bragg's law

The Bragg approach to diffraction is to regard crystals as built up in layers or planes such that each acts as a semi-transparent mirror. Fig. 3.5 shows the derivation of Bragg's law. Two X-ray beams, 1 and 2, are reflected from the adjacent planes, A and B, with the angle of reflection equal to the angle of incidence. We wish to know under what condition the reflected beams 1' and 2' are in phase.

$$xy = yz = d \sin \theta$$

$$xyz = 2d \sin \theta = n \lambda$$

$$2d \sin \theta = n \lambda \quad \text{Bragg's law}$$

Because real crystals contains thousands of planes, cancellation of the reflected beams is usually complete if the incident angle is incorrect by more than a few tenths of a degree.

It is customary to set  $n$  equal to 1 for Bragg's law. For situations where, say,  $n = 2$ , the  $d$ -spacing is instead halved by doubling up the number of planes. (Note that  $2\lambda = 2d \sin \theta$  is equivalent to  $\lambda = 2(d/2) \sin \theta$ )

In some cases the planes derived from Bragg's law correspond to layers of atoms, but this is not generally the case. The semi-transparent layers are a concept rather than a physical reality. The atoms do not reflect X-rays but scatter or diffract them in all directions. Nevertheless, the highly simplified treatment in deriving Bragg's law gives exactly the same answers as are obtained by a rigorous treatment. We are fortunate to have such a simple and picturesque, albeit inaccurate, way to describe a very complicated process.

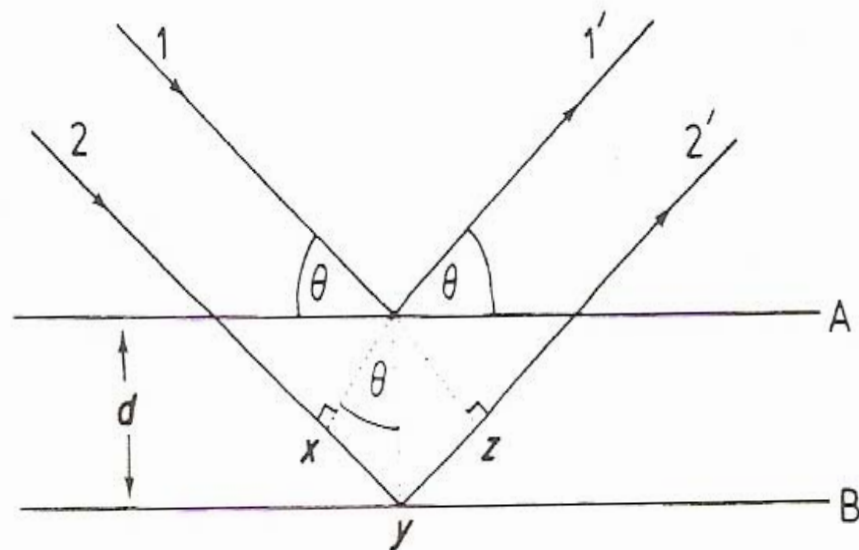


Fig. 3.5 Derivation of Bragg's law

#### d) X-ray diffraction methods

The X-ray diffraction experiment requires an X-ray source, the sample, and a detector to pick up the diffracted X-rays (Fig. 3.6). Three variables govern the different X-ray techniques:

(a) radiation— monochromatic or variable  $\lambda$

(b) sample— single crystal, powder or a solid piece

(c) detector— radiation counter or photographic film

Fig. 3.7 summarizes the most important techniques. Monochromatic radiation is nearly always used (the Laue method is used by metallurgists).

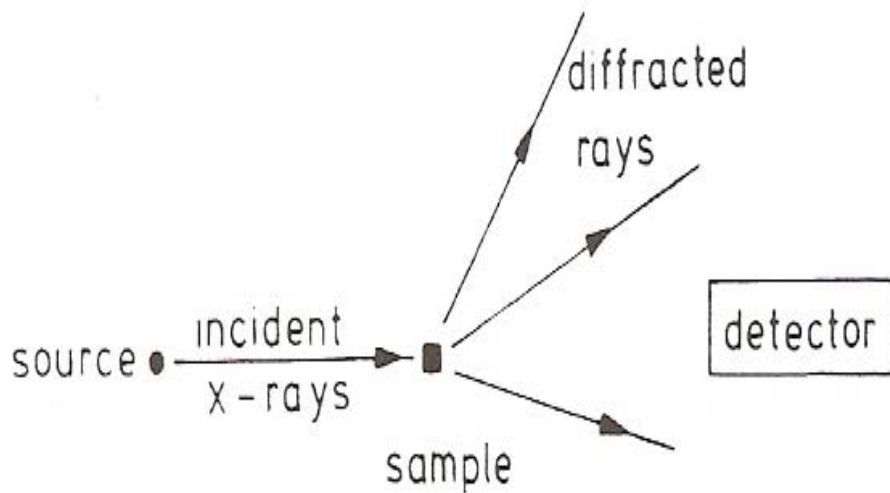


Fig. 3.6 The X-ray diffraction experiment

<i>WAVELENGTH</i>	<i>SAMPLE</i>	<i>DETECTOR</i>	<i>METHOD</i>
Fixed	Powder	Counter	Diffractometer
		Film	{ Debye-Scherrer Guinier (Focusing)
Variable	Single crystal	Film	{ Rotation (Oscillation) Weissenberg Precession (Buerger)
		Counter	Automatic Diffractometer
Variable	Solid piece	Film	Laue

Fig. 3.7 The different X-ray diffraction techniques

### e) The powder method– principles and uses

Fig. 3.8 shows that a monochromatic beam of X-rays strikes at a finely powdered sample (randomly oriented). For each set of planes, at least some crystals must be oriented at the Bragg angle,  $\theta$ , to the incident beam and diffraction occurs. The diffracted beams may be detected either by surrounding the sample with a strip of photographic film (Debye-Scherrer) or by using a movable detector connected to a computer (diffractometer).

The original method (Debye-Scherrer) is instructive (though is little used nowadays). For any set of lattice planes, the diffracted radiation forms the surface of a cone (Fig. 3.9, no restriction on the angular orientation). If the Bragg angle is  $\theta$ , the angle between the diffracted and undiffracted beams is  $2\theta$  and angle of the cone is  $4\theta$ . The cones are detected by a strip of film wrapped around the sample (Fig. 3.8). Each cone intersects the film as two arcs (Fig. 3.10), which are symmetrical about the two holes (for incident entry and undiffracted exit).

To obtain d-spacing,

$$S/2\pi R = 4\theta/360$$

where  $S$  is the separation between pairs of corresponding arcs,  $R$  is the film radius.  $2\theta$  and therefore  $d$  ( $2d \sin\theta = n\lambda$ ) can be obtained. The disadvantages: long exposure time (6 to 24 h) and low resolution. A finer collimator (for beam focusing) is needed.

Diffractometry gives a series of peaks on a PC (or a strip chart). Both peak positions (d-spacings) and intensities are important for phase analysis.

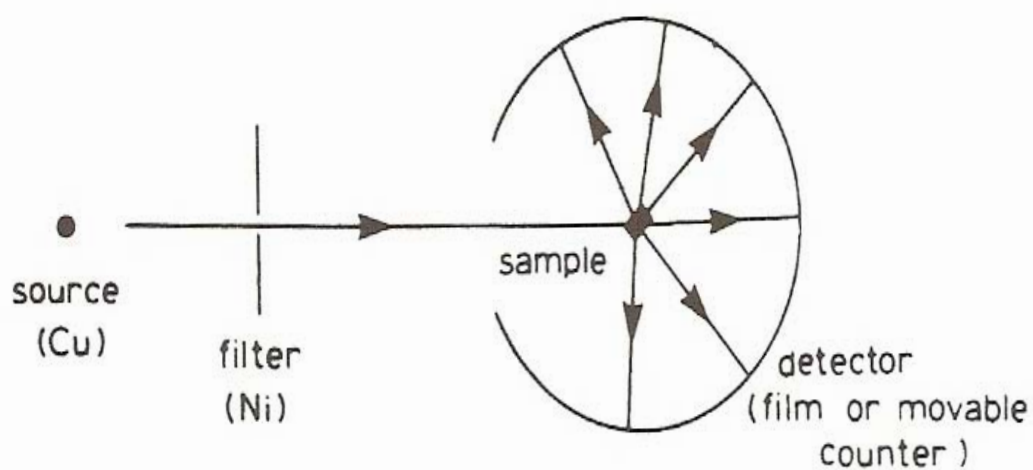


Fig. 3.8 The powder method

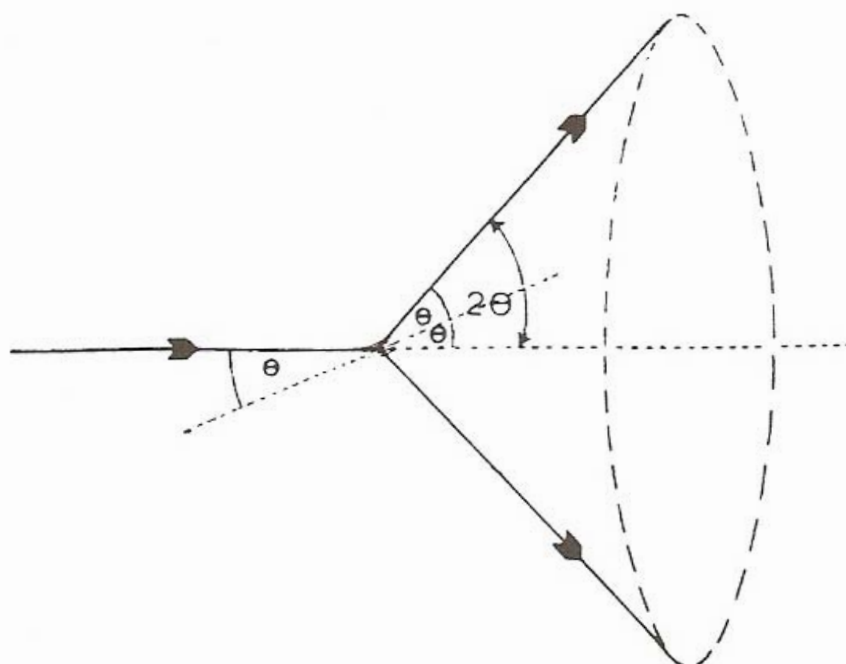
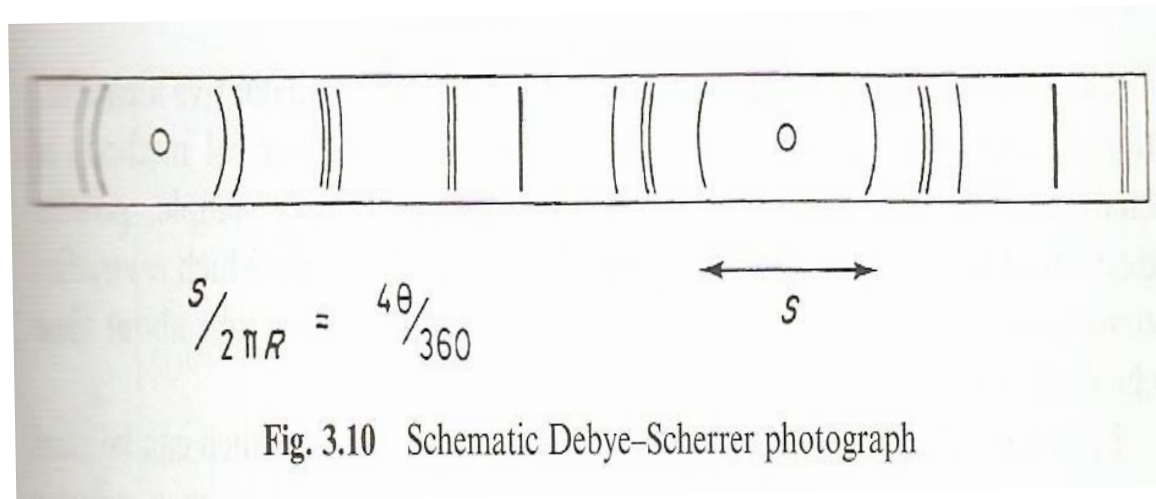


Fig. 3.9 Formation of a cone of diffracted radiation

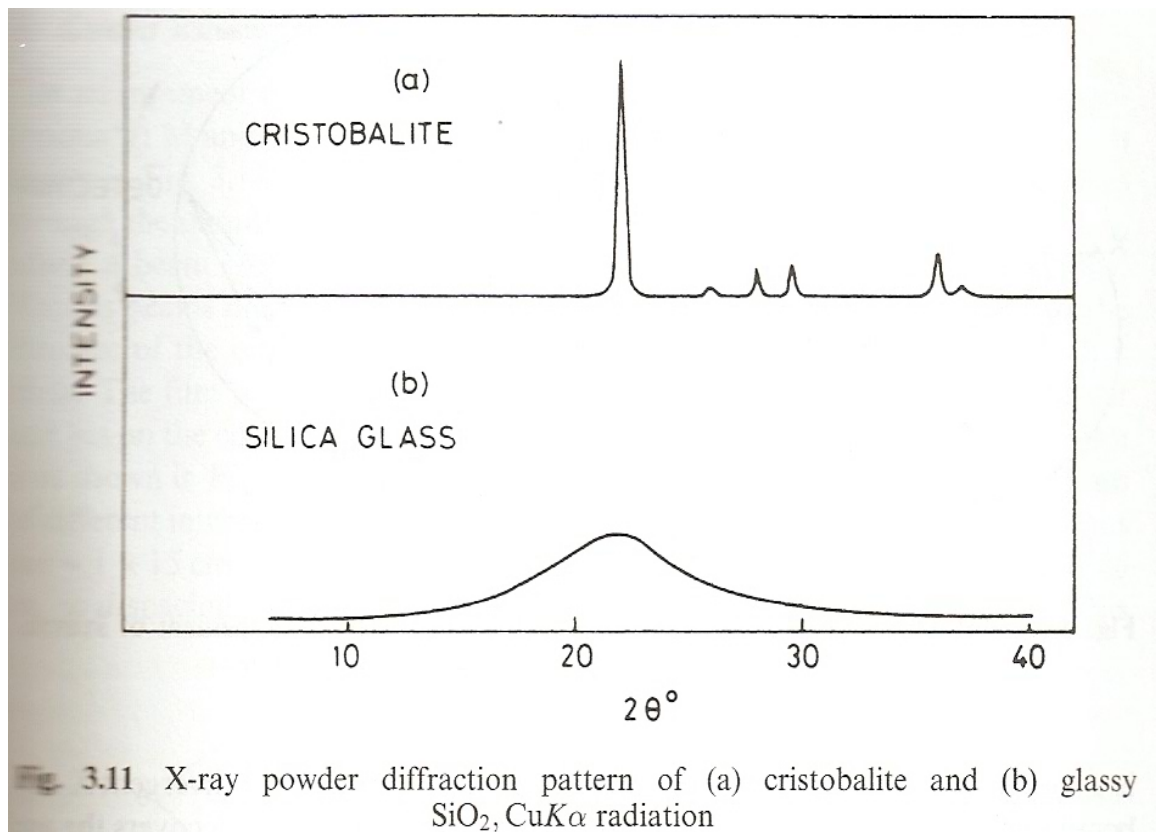


*Powder Diffraction File* (International Center for Diffraction Data, USA), previously known as the ASTM or JCPDS file is an invaluable reference source for the identification of unknown crystalline materials. The file contains about 35, 000 materials. Materials are classified either according to their most intense peaks or according to the first eight lines. Problems arise if the material is not included in the file or if the material contains lines from more than one phase.

#### f) Powder diffractometer

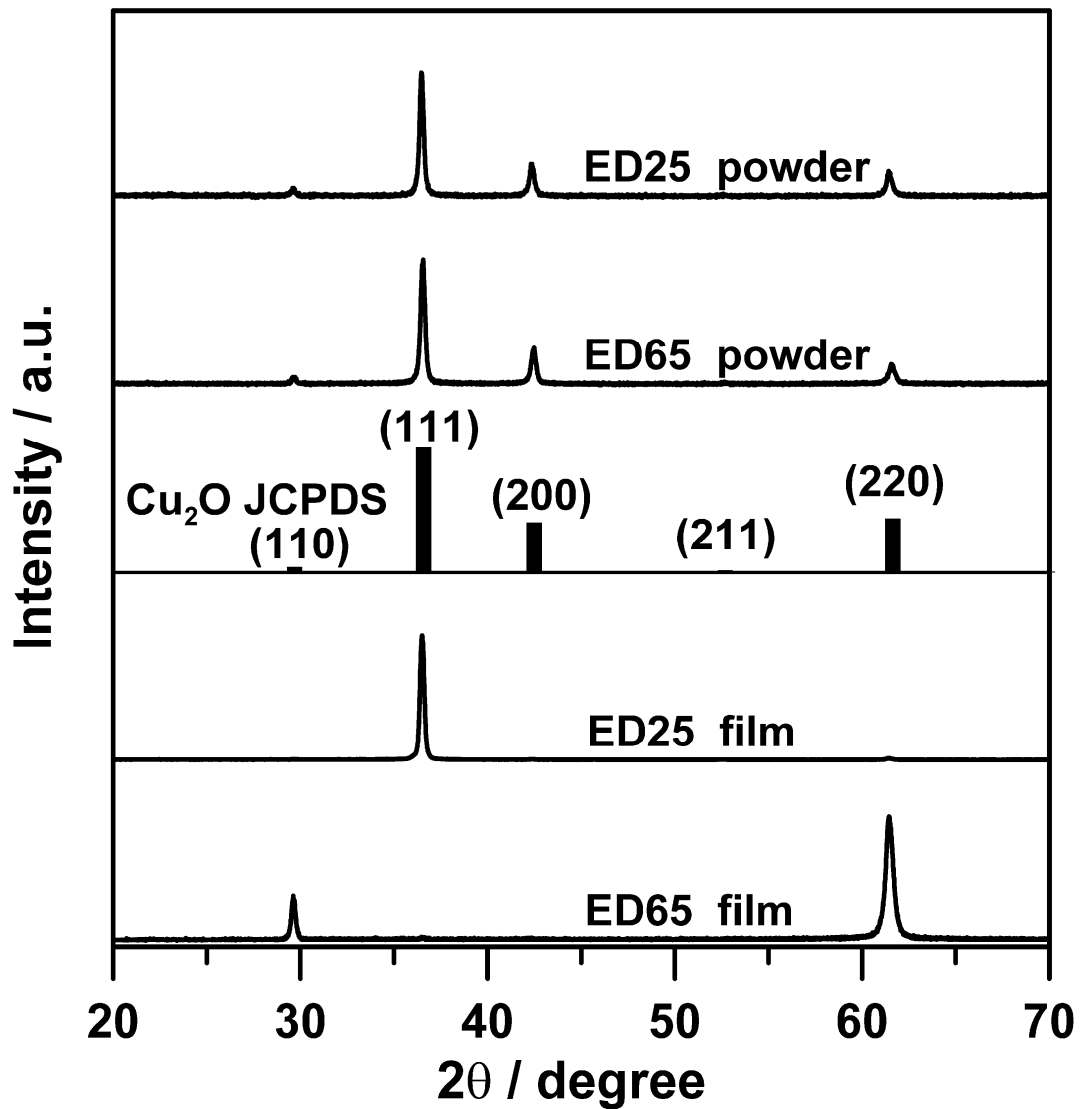
The powder diffractometer has a proportional, scintillation or Geiger counter which scans a range of  $2\theta$  values at constant angular velocity ( $2\theta = 10-80^\circ$  usually sufficient).

Fig. 3.11. A typical diffractometer trace. The scanning speed of the counter is usually  $2^\circ 2\theta \text{ min}^{-1}$  (about 30 min to obtain a trace). Intensities are taken as either peak heights or peak areas (more accurate).



For accurate d-spacings, an internal standard (such as KCl, whose d-spacings are known accurately) is mixed in with the sample. A correction factor, which may vary with  $2\theta$ , is obtained from the discrepancy between the observed and true d-spacing of the standard.

Sample forms: a. thin layers of fine powder sprinkled onto a glass slide smeared with vaseline; b. thin flakes pressed onto a glass slide. A random arrangement of crystal orientations is important. If not random, preferred orientation exists and can introduce errors. Preferred orientation is a serious problem for materials that crystallize in a characteristic, very non-spherical shape.



Powder X-ray diffraction patterns of the ED25 and ED65 Cu<sub>2</sub>O powders (upper section) and the films (lower section). The standard diffraction pattern of Cu<sub>2</sub>O from JCPDS is provided at the middle of this figure.

### g) Focusing of X-rays: theorem of a circle

The incident and diffracted beams are inevitably divergent and of low intensity. Using a convergent X-ray beam gives a dramatic improvement in resolution and significantly reduces the exposure times. Fig. 3.12a

shows the use of geometric properties of the circle to obtain a convergent X-ray beam. All angles subtended 對向,包住 on the circle circumference by the arc XY are equal,  $\angle XCY = \angle XC'Y = \angle XC''Y = \alpha$ . A sample covers the arc between C and C' such that the diffracting planes are tangential to the circle. Suppose X is a source of X-rays and XC and XC' represent the extremities of a divergent X-ray beam, the diffracted beam, CY and C'Y, will focus to a point at Y (Fig. 3.12b, detector Y position varies).

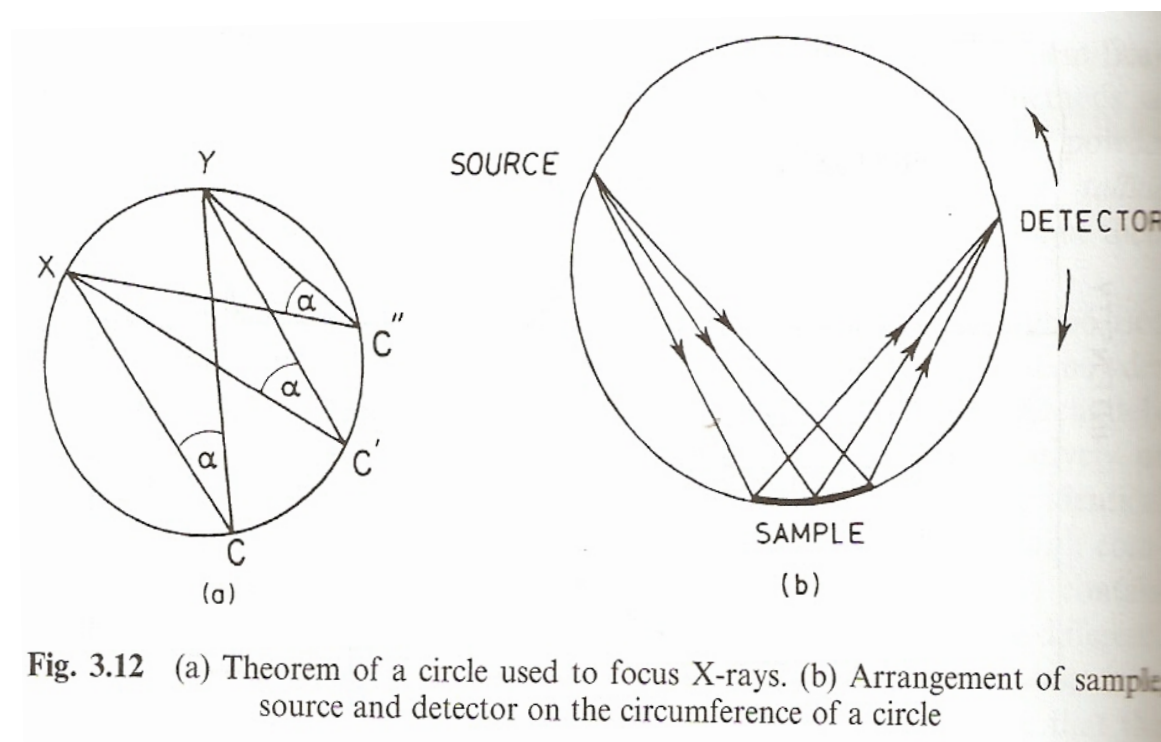


Fig. 3.12 (a) Theorem of a circle used to focus X-rays. (b) Arrangement of sample, source and detector on the circumference of a circle

## h) Crystal monochromators

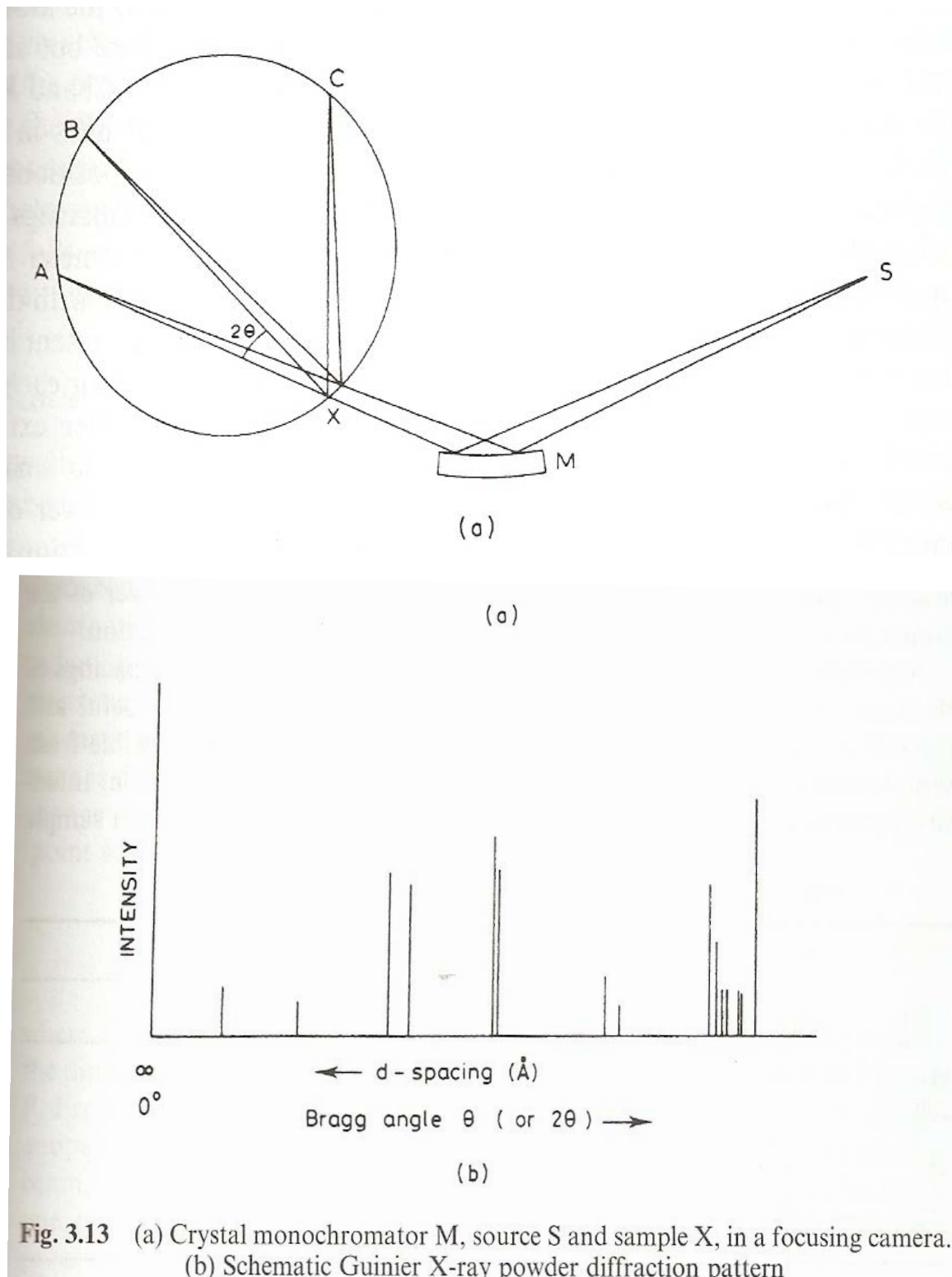
A crystal monochromator serves two functions: to give highly monochromatic radiation and to produce an intense, convergent X-ray beam. There are several sources of background scattering in diffraction experiments.  $K_{\alpha}$  radiation may be separated from the rest by the use of filters, or, better, by a crystal monochromator.

A crystal monochromator consists of a large single crystal of, e.g. quartz, oriented such that one set of planes which diffracts strongly is at the Bragg angle to the incident beam. This Bragg is calculated for  $\lambda_{K\alpha 1}$  and so only the  $K_{\alpha 1}$  rays are diffracted, giving monochromatic radiation. To improve the efficiency, the crystal monochromator is bent, in which case a divergent X-ray beam is diffracted (according to the circle theorem) to give an intense, monochromatic and divergent beam.

### **i) Guinier focusing cameras**

Fig. 3.13a. A Guinier camera uses a crystal monochromator M and also makes use of the circle theorem. A convergent beam from M passes through sample at X. Radiation that is not diffracted comes to a focus at A. Various beams diffracted by the sample focus at B, C, ... etc.

We know from the theorem of the circle that all radiations diffracted by the sample at  $2\theta$  focus at B. A film placed in a cassette which lies on the circle ABC. The film records the diffraction results (Fig. 3.13b)



**j) A powder pattern of a crystalline phase is its ‘fingerprint’**

Two main factors determine powder pattern: (a) the size and shape of the unit cell, (b) the atomic number and position of the atoms in the cell. ∴

two materials have the same crystal structure but certainly will have distinct powder patterns.

Table 3.3. KF, KCl and KI have the rock salt structure, but both the positions and intensities of the lines are different in each. Different positions are due to different unit cell sizes and different intensities are due to different atomic number and therefore different scattering powers.

Table 3.3 *X-ray powder diffraction patterns for potassium halides*

<i>(hkl)</i>	KF, $a = 5.347 \text{ \AA}$		KCl, $a = 6.2931 \text{ \AA}$		KI, $a = 7.0655 \text{ \AA}$	
	$d(\text{\AA})$	$I$	$d(\text{\AA})$	$I$	$d(\text{\AA})$	$I$
111	3.087	29	—	—	4.08	42
200	2.671	100	3.146	100	3.53	100
220	1.890	63	2.224	59	2.498	70
311	1.612	10	—	—	2.131	29
222	1.542	17	1.816	23	2.039	27
400	1.337	8	1.573	8	1.767	15

A powder pattern has two characteristic features: the d-spacings of the lines and their intensity. The likelihood of two materials have the same cell parameters and d-spacings decreases considerably with decreasing crystal symmetry. Cubic materials have only one variable,  $a$ . Triclinic powder patterns have six variables,  $a$ ,  $b$ ,  $c$ ,  $\alpha$ ,  $\beta$ ,  $\gamma$ . Problems of identification are most likely to be experienced with high symmetry.

### k) Intensities

Intensities are important: (a) quantitative measurements are necessary to solve crystal structure, (b) intensity data are needed in the powder fingerprint method to identify unknowns with the *Powder Diffraction File*. Two topics: the intensity scattered by individual atoms and the resultant intensity scattered from the large number of atoms in a crystal.

*1) Scattering of X-rays by an atom: atomic scattering factor*

An incident X-ray beam is an electromagnetic wave with an oscillating electric field, which can set each electron of an atom into vibration. A vibrating electron emits radiation which is in phase or coherent with the incident X-ray beam. Coherent scattering may be likened to an elastic collision between the wave and the electron (no energy loss and thus no  $\lambda$  change). The electrons become secondary sources of X-rays.

$$I_P \propto 1/2 (1 + \cos^2 2\theta) \quad \text{Thomson equation} \quad (3.5)$$

$I_P$ : scattered density at any point P;  $2\theta$ : angle between the incident beam and the diffracted. From the Thomson equation, the scattered beams are most intense when parallel or antiparallel to the incident and are weakest when at  $90^\circ$   $2\theta$ . The Thomson equation is also known as the polarization factor.

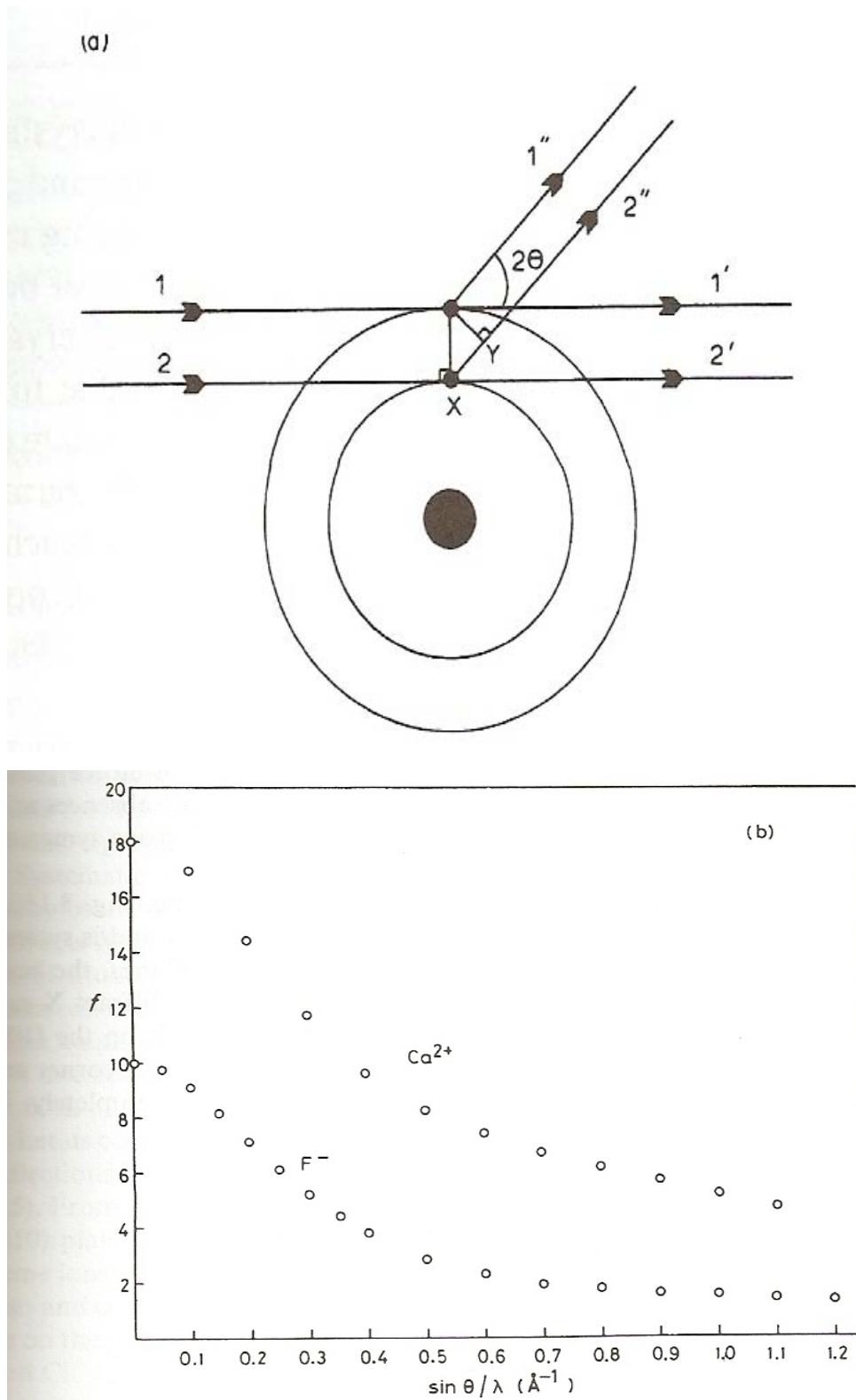
Compton scattering: caused by interaction between X-rays and more loosely held valence electrons. X-rays lose energy and the scattered are of longer wavelength (no longer in phase, like background white radiation). This is an important effect with the lighter elements, being especially deleterious to the patterns of organic materials.

Fig. 3.14a. The X-ray scattered by an atom are the resultant of the wave scattered by each electron in the atom. Like beams 1' and 2', all electrons scatter in phase irrespective of their position. The scattering factor (form factor,  $f$ ) of an atom is proportional to its atomic number,  $Z$ , or, more strictly, to the number of electrons possessed by that atom.

For scattering at some  $2\theta$ , a phase difference  $XY$  exists between beams 1'' and 2''. Because the distances between electrons within an atom are short,  $\lambda < XY$ , destructive interference occurs and apparently the scattered intensity decreases with increasing  $2\theta$  (因為  $XY$  increase, 但仍遠小於 $\lambda$ ). The cancellation effect is also greater for smaller  $\lambda$ . Fig. 3.14b show the variation of the form factor with  $\sin\theta/\lambda$ .

Consequences of form factor  $f = \text{funct.}(Z, \sin\theta/\lambda)$

Powder patterns are weak at high angles. It is difficult to locate light atoms because their diffracted radiation is so weak. H cannot be located unless all others present are extremely light. Atoms that have as many electrons as oxygen can be located easily unless a very heavy atom (such as uranium) is present. Structures that have a considerable number of atoms have similar atomic number, e.g. large organic molecules with C, N and O, or aluminosilicates with Al and Si, are difficult to solve or distinguish. Using neutrons can solve the problem because the neutron form factors are not a simple function of  $Z$ . Light atoms, Li and H, are often strong neutron scatterers.



**Fig. 3.14** (a) Scattering of X-rays by electrons in an atom. (b) Form factors of Ca<sup>2+</sup> and F<sup>-</sup>

## 2) Scattering of X-ray by a crystal— systematic absence

In principle, each set of lattice planes can give rise to a diffracted beam

(Table 3.4 for an orthorhombic cell). In practice, the intensity by certain sets may be zero. Systematic absences arise if the lattice type is non-primitive (I, F, etc) or if elements of space symmetry are present.

Table 3.4 *Calculated d-spacings for an orthorhombic cell, for  $a = 3.0, b = 4.0, c = 5.0 \text{ \AA}$*

$hkl$	$d (\text{\AA})$	$hkl$	$d (\text{\AA})$
001	5.00	101	2.57
010	4.00	110	2.40
011	3.12	111	2.16
100	3.00		

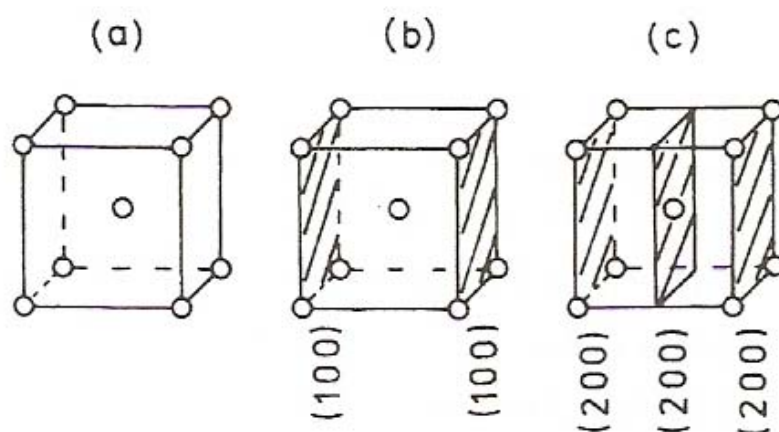


**Fig. 3.15** (a) *bcc*  $\alpha$ -Fe, (b) (100) planes, (c) (200) planes

Consider  $\alpha$ -Fe, Fig. 3.15a, which is bcc. Reflection from the (100) planes has zero intensity and is systematically absent. This is because, at the Bragg angle for these planes, the body center atom planes diffract X-ray exactly  $180^\circ$  out of phase (指 X-ray 的波動而非  $2\theta$ ) relative to the (100) planes. In

contrast, a strong 200 reflection is observed (Fig. 3.15c). Similarly, the 110 reflection is observed where 111 is absent in  $\alpha$ -Fe. Table 3.5 shows a simple characteristic formula for systematic absence. For bcc, reflections, for which  $h+k+l$  is odd, are absent (e.g. 100, 111, 320).

Two conditions must be met for systematic absence: the diffracted beams must be out of phase (by  $\lambda/2$  or  $\pi$ ) and of the same amplitude (determined by scattering powers,  $f$ ).

Table 3.5 *Systematic absences due to lattice type*

Lattice type	Rule for reflection to be observed*
Primitive, P	None
Body centred, I	$hkl; h + k + l = 2n$
Face centred, F	$hkl; h, k, l$ either all odd or all even
Side centred, e.g. C	$hkl; h + k = 2n$
Rhombohedral, R	$hkl; -h + k + l = 3n$ or $(h - k + l = 3n)$

\* If space symmetry elements are present, additional rules may apply. These are not dealt with here.

Consider NaCl, a rock salt, in which either Na or Cl is fcc. According to Table 3.5, (110) is systematic absent. Fig. 3.16a shows that (110) planes have Na and Cl ions but equal numbers of the ions are midway between the planes. Complete cancellation occurs. For the (111) planes, Na ions lie on the planes and Cl ions lie midway between them. Since they have different scattering powers the destructive interference is only partial. The intensity of (111) reflection is related to the difference in atomic number

of anion and cation. Since  $K^+$  and  $Cl^-$  are isoelectronic, the (111) intensity of KCl is zero. The intensity order:

$$KCl < KF < KBr < KI \quad (\text{Table 3.3})$$

The (100) reflection is observed with primitive cubic CsCl because the scattering powers of  $Cs^+$  and  $Cl^-$  are different.

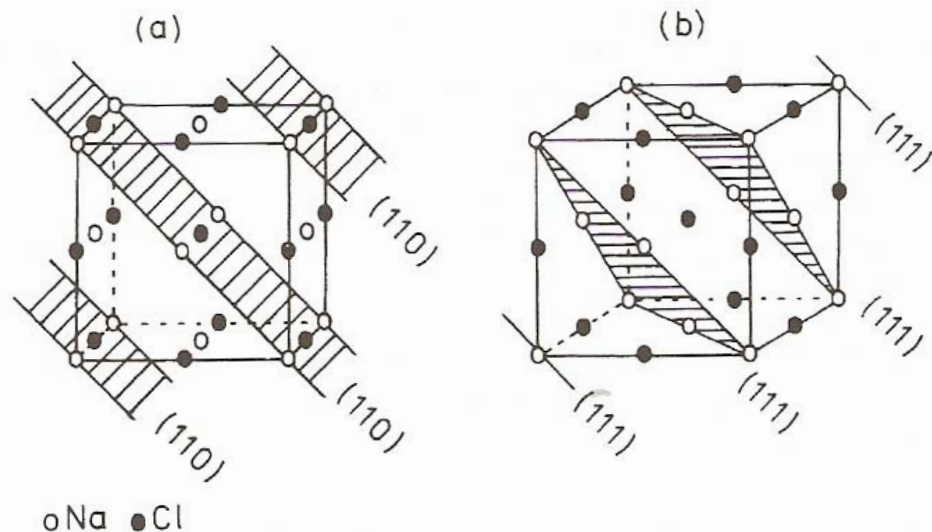


Fig. 3.16 (a) (110) and (b) (111) planes in NaCl

### 3) General formula for phase difference, $\delta$

Fig. 3.17a shows two (100) planes of an orthogonal unit cell. A and A' at the origin of adjacent unit cells. For the 100 reflection, A and A' scatter in phase because their phase difference is exactly one wavelength,  $2\pi$  radians. B situated halfway between adjacent (100) planes has fractional coordinate of  $x = 1/2$ . The phase difference between A and B is  $1/2 \times 2\pi = \pi$ , i.e. out of phase (Fig. 3.17b). Atom C situated at  $x$  has a phase difference relative to A of  $2\pi x$ .

Consider the (200) reflection, Fig. 3.17c. Since  $d_{200} = (1/2)d_{100}$ , the Bragg's law gives  $\sin\theta_{200} = 2\sin\theta_{100}$ ,  $\therefore \theta_{200} \gg \theta_{100}$ . Atoms A and B have

phase difference of  $2\pi$  for the (200) reflection and  $\pi$  for the (100) reflection. Thus, halving  $d$  is to double the relative phase difference between two atoms. A and C have a phase difference of  $2 \cdot 2\pi x$  for the (200) reflection.

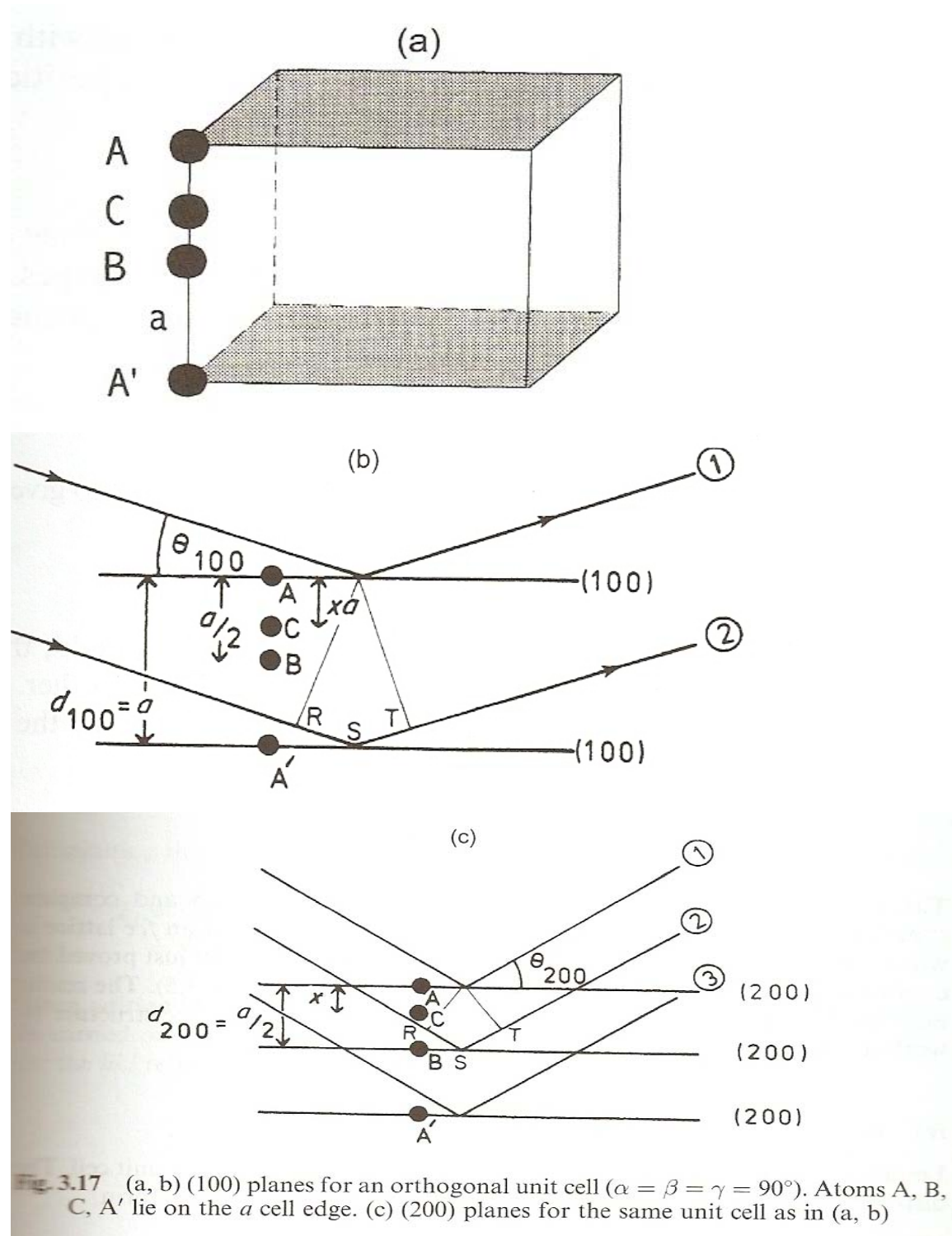


Fig. 3.17 (a, b) (100) planes for an orthogonal unit cell ( $\alpha = \beta = \gamma = 90^\circ$ ). Atoms A, B, C, A' lie on the  $a$  cell edge. (c) (200) planes for the same unit cell as in (a, b)

For the general case of an  $h00$  reflection, the phase difference,  $\delta$ , between

A and C is given by

$$\delta = 2\pi xh$$

The phase difference between atoms depends on: 1. the indices of the reflection; 2. the coordinates of the atoms.

In 3D, for reflection indices  $(hkl)$  the phase difference between the origin and an atom at  $(x,y,z)$  is given by

$$\delta = 2\pi(xh + yk + zl)$$

Let us use this equation for fcc  $\gamma$ -Fe with atoms at corners and face centers,

$$0,0,0; \quad \frac{1}{2}, \frac{1}{2}, 0; \quad \frac{1}{2}, 0, \frac{1}{2}; \quad 0, \frac{1}{2}, \frac{1}{2}$$

The phase differences  $\delta$  for the four positions relative to the origin are

$$0; \quad \pi(h + k); \quad \pi(h + l); \quad \pi(k + l)$$

If  $h$ ,  $k$ , and  $l$  are either all even or all odd, the phases are in multiples of  $2\pi$ , and are in phase with each other. If  $h$  is odd and  $k$  and  $l$  are even, the four phases reduce to

$$0; \quad (2n + 1)\pi; \quad (2n + 1)\pi; \quad 2n\pi$$

The first and last are out of phase with the middle two and complete cancellation occurs. This example shows the condition for systematic absence due to face centering (Table 3.5).

#### 4) Intensities and structure factors

Considering any atom  $j$  in the unit cell, the diffracted wave of amplitude  $f_j$  and phase  $\delta_j$  is a sine wave of

$$F_j = f_j \sin(\omega t - \delta_j)$$

The waves diffracted from each atom in the cell have the same angular

frequency,  $\omega$ , but may differ in  $f$  and  $\delta$ .

In complex notation,

$$F_j = f_j (\cos\delta_j + i \sin\delta_j) \quad \text{or} \quad F_j = f_j \exp(i\delta_j) \quad \text{where } i = \sqrt{-1}$$

The intensity of a wave is obtained by multiplying the equation for the wave by its complete conjugate; i.e.

$$I \propto f_j \exp(i\delta_j) \cdot f_j \exp(-i\delta_j)$$

$$I \propto f_j^2$$

Alternatively,

$$[f_j (\cos\delta_j + i \sin\delta_j)][f_j (\cos\delta_j - i \sin\delta_j)] = f_j^2(\cos^2\delta_j + \sin^2\delta_j) = f_j^2$$

Substituting the expression for  $\delta$ ,

$$\begin{aligned} F_j &= f_j \exp 2\pi i(hx_j + ky_j + lz_j) \\ &= f_j [\cos 2\pi(hx_j + ky_j + lz_j) + i \sin 2\pi(hx_j + ky_j + lz_j)] \end{aligned}$$

The structure factor or structure amplitude,  $F_{hkl}$ , for the hkl reflection; i.e.

$$F_{hkl} = \sum_{j=1 \rightarrow n} [f_j \exp(i\delta_j)]$$

OR

$$F_{hkl} = \sum_j f_j (\cos \delta_j + i \sin \delta_j)$$

The intensity of the diffracted beam  $I_{hkl}$  is proportional to  $|F_{hkl}|^2$  and is obtained from

$$\begin{aligned} I_{hkl} \propto |F_{hkl}|^2 &= \left[ \sum_j f_j (\cos \delta_j + i \sin \delta_j) \right] \left[ \sum_j f_j (\cos \delta_j - i \sin \delta_j) \right] \\ &= \sum_j (f_j \cos \delta_j)^2 + \sum_j (f_j \sin \delta_j)^2 \end{aligned}$$

This latter is a very important formula in crystallography because, using it, the **intensity of any  $hkl$**  reflection may be calculated from a knowledge of the atomic coordinates in the unit cell. Let us see one example of its use. Calcium fluoride,  $\text{CaF}_2$ , has the fluorite structure with atomic coordinates in the *fcc* unit cell:

$$\begin{array}{l} \text{Ca} \quad 0, 0, 0 \quad \frac{1}{2}, \frac{1}{2}, 0 \quad \frac{1}{2}, 0, \frac{1}{2} \quad 0, \frac{1}{2}, \frac{1}{2} \\ \text{F} \quad \frac{1}{4}, \frac{1}{4}, \frac{1}{4} \quad \frac{1}{4}, \frac{1}{4}, \frac{3}{4} \quad \frac{1}{4}, \frac{3}{4}, \frac{1}{4} \quad \frac{3}{4}, \frac{1}{4}, \frac{1}{4} \\ \quad \frac{3}{4}, \frac{3}{4}, \frac{1}{4} \quad \frac{3}{4}, \frac{1}{4}, \frac{3}{4} \quad \frac{1}{4}, \frac{3}{4}, \frac{3}{4} \quad \frac{3}{4}, \frac{3}{4}, \frac{3}{4} \end{array}$$

Substitution of these coordinates into (3.13), yields

$$\begin{aligned} F_{hkl} = & f_{\text{Ca}} [\cos 2\pi(0) + \cos \pi(h+k) + \cos \pi(h+l) + \cos \pi(k+l)] \\ & + if_{\text{Ca}} [\sin 2\pi(0) + \sin \pi(h+k) + \sin \pi(h+l) \\ & + \sin \pi(k+l)] + f_{\text{F}} [\cos \pi/2(h+k+l) \\ & + \cos \pi/2(h+k+3l) + \cos \pi/2(h+3k+l) \\ & + \cos \pi/2(3h+k+l) + \cos \pi/2(3h+3k+l) \\ & + \cos \pi/2(3h+k+3l) + \cos \pi/2(h+3k+3l) \\ & + \cos \pi/2(3h+3k+3l)] + if_{\text{F}} [\sin \pi/2(h+k+l) \\ & + \sin \pi/2(h+k+3l) + \sin \pi/2(h+3k+l) + \sin \pi/2(3h+k+l) \\ & + \sin \pi/2(3h+3k+l) + \sin \pi/2(3h+k+3l) \\ & + \sin \pi/2(h+3k+3l) + \sin \pi/2(3h+3k+3l)] \end{aligned}$$

Since the fluorite structure is *fcc*,  $h, k$  and  $l$  must be all odd or all even for an observed reflection; for any other combination,  $F = 0$  (try it!). Consider the reflection 202:

$$\begin{aligned} F_{202} = & f_{\text{Ca}} (\cos 0 + \cos 2\pi + \cos 4\pi + \cos 2\pi) \\ & + if_{\text{Ca}} (\sin 0 + \sin 2\pi + \sin 4\pi + \sin 2\pi) \\ & + f_{\text{F}} (\cos 2\pi + \cos 4\pi + \cos 2\pi + \cos 4\pi + \cos 4\pi + \cos 6\pi \\ & + \cos 4\pi + \cos 6\pi) + if_{\text{F}} (\sin 2\pi + \sin 4\pi + \sin 2\pi + \sin 4\pi + \sin 4\pi \\ & + \sin 6\pi + \sin 4\pi + \sin 6\pi) \end{aligned}$$

That is,

$$\begin{aligned} F_{202} = & f_{\text{Ca}} (1 + 1 + 1 + 1) + if_{\text{Ca}} (0 + 0 + 0 + 0) \\ & + f_{\text{F}} (1 + 1 + 1 + 1 + 1 + 1 + 1 + 1) \\ & + if_{\text{F}} (0 + 0 + 0 + 0 + 0 + 0 + 0 + 0) \end{aligned}$$

i.e.

$$F_{202} = 4f_{\text{Ca}} + 8f_{\text{F}}$$

The 202 reflection in  $\text{CaF}_2$  has a d-spacing of 1.929 Å ( $a = 5.464$  Å).

$$\theta_{202} = 23.6^\circ \text{ and } \sin\theta/\lambda = 0.259 \text{ for } \lambda = 1.5418 \text{ Å (Cu K}\alpha\text{)}$$

Form factors for Ca and F are given in Fig. 3.14b for  $\sin\theta/\lambda = 0.259$

$$f_{\text{Ca}} = 12.65 \quad \text{and} \quad f_{\text{F}} = 5.8$$

$$\rightarrow F_{202} = 97$$

Table 3.6 shows the observed  $F_{\text{hkl}}$  values and the calculated values after scaling. In solving unknown structure, the objective is always to obtain a model structure (by assuming atomic coordinates) for which the  $F_{\text{hkl}}^{\text{calc}}$  values are in good agreement with experimental  $F_{\text{hkl}}^{\text{obs}}$  values.

#### 5) R-factors and structure determination

Table 3.6 shows the values of  $F_{\text{hkl}}^{\text{calc}}$  for the first five lines in the  $\text{CaF}_2$  powder pattern.

For  $F_{\text{hkl}}^{\text{obs}} = \sqrt{I_{\text{corr}}}$ , the experimental intensities are corrected for  $L_p$  factor and multiplicity to give  $I_{\text{corr}}$ . In order to compare  $F_{\text{hkl}}^{\text{obs}}$  and  $F_{\text{hkl}}^{\text{calc}}$ , the  $F_{\text{hkl}}^{\text{obs}}$  values are scaled such that  $\sum F_{\text{hkl}}^{\text{obs}} = \sum F_{\text{hkl}}^{\text{calc}}$ . Multiplication of each  $F_{\text{hkl}}^{\text{obs}}$  value by 141 gives the scale values listed in Table 3.6.

The measure of agreement between the scaled  $F_{\text{hkl}}^{\text{obs}}$  and  $F_{\text{hkl}}^{\text{calc}}$ , is given by the residual factor or R-factor defined by

$$R = \frac{\sum \|F^{\text{obs}} - F^{\text{calc}}\|}{\sum |F^{\text{obs}}|}$$

An R-factor of 0.15 (or 15%) is obtained for the data in Table 3.6. Usually, when R is less than 0.1 to 0.2, the proposed structure is essentially correct. A structure which has been solved fully using good quality intensity data has R typically in the range of 0.02 to 0.06.

Table 3.6 Structure factor calculations for  $\text{CaF}_2$ : X-ray powder diffraction

$d$ (Å)	$hkl$	$I$	Multiplicity*	$I/(\text{multiplicity} \times L_p)^\dagger$	$F^{\text{obs}}$	$F^{\text{calc}}$	$F^{\text{obs}}$ scaled	$\ F^{\text{obs}}  -  F^{\text{calc}}\ $
3.143	111	100	8	0.409	0.640	67	90	23
1.929	202	57	12	0.476	0.690	97	97	0
1.647	311	16	24	0.098	0.313	47	44	3
1.366	400	5	6	0.193	0.439	75	62	13
1.254	331	4	24	0.047	0.217	39	31	8

$$\sum F^{\text{obs scaled}} = 324$$

$$\sum \|F^{\text{obs}}| - |F^{\text{calc}}\| = 47$$

$$R = \frac{\sum |\Delta F|}{\sum F^{\text{obs}}} = \frac{47}{324} = 0.15$$

\* The multiplicity of an X-ray powder line is the number of equivalent sets of planes that diffract at the same Bragg angle. Thus, overlapping with 111 are  $\bar{1}\bar{1}1$ ,  $1\bar{1}\bar{1}$ ,  $11\bar{1}$ ,  $\bar{1}11$ ,  $11\bar{1}$  and  $\bar{1}\bar{1}1$ , where a negative index indicates that a negative crystallographic direction was used in defining it.

† The Lorentz polarization factor,  $L_p$ , is an angular correction factor that includes the effect of equation (3.5) and certain instrumental factors. Available from standard tables.